**Applied Physics Frontier**
November 2013, Volume 1, Issue 4, PP.32-44

# A Novel Finite Volume Scheme with Geometric Average Method for Radiative Heat Transfer Problems*

***Cunyun Nie[1†], Haiyuan Yu [2]***

1. Department of Mathematics and Physics, Hunan Institution of Engineering, Xiangtan , Hunan 411104 China

2. Hunan Key Laboratory for Computation & Simulation in Science and Engineering and Key Laboratory of Intelligent Computing & Information Processing of Ministry of Education, Xiangtan University, Hunan 411105, China

†Email: ncy1028@gmail.com, nie272@aliyun.com

***Abstract***

We construct a novel finite volume scheme by innovatively introducing the weighted geometric average method for solving three multi-material radiative heat transfer problems, and compare it with the weighted arithmetic and harmonic average methods, respectively. We also put forward the effect of the convexity of nonlinear diffusion functions. Then, we present a cylinder symmetric finite volume element (SFVE) scheme for the three-dimensional problem by transferring it to a two-dimensional one with the axis symmetry. Numerical experiments reveal that the convergent order is less than two, and numerical stimulations are valid and rational, and confirm that the new scheme is agreeable for solving radiative heat transfer problems.

***Keywords: Finite Volume Scheme; Weighted Geometric Average Method; Radiative Heat Transfer Problems; Convexity of Diffusion Functions***

## 1 INTRODUCTION

Numerical approximations of second order elliptic or parabolic problems with discontinuous coefficients are often encountered in material sciences and fluid dynamics. Discontinuous diffusion coefficients correspond to multi-material heat transfer problem which is one of important interface problems [1,2,3,4]. Jafari presented a 2-D transient heat transfer finite element analysis for some multi-physics problem in [1]. Pei and his colleagues obtained satisfactory numerical results in the integrated simulation of ignition hohlraum by Lared-H code in the literature [2], and the Arbitrary Lagrangian-Eulerian method was used to treat the large deformation problem and multi-material cells were introduced when the material interface is severely distorted. James and Chen discussed finite element methods for interface problems, and obtained the optimal $L^2$-norm and energy-norm error estimates for regular problems when the interfaces are of arbitrary shape but are smooth in [3,4]. The harmonic average was promoted by Patankar [5]. It was often designed to solve heat transfer problems involving multiple material properties. Recently, in [6], Kadioglu and his workers has taken a comparative study of the harmonic and arithmetic averaging of diffusion coefficients for nonlinear heat conduction problems, and revealed that the harmonic average is not always better than the arithmetic one. The weight harmonic average finite volume and finite difference schemes were discussed for some interface problems in some other literatures [7,8,9,10].

It is well-known that the engineers are usually zealous for the arithmetic and harmonic average methods for interface problems, but ignore the geometric average one. In this paper, we construct a novel finite volume scheme for solving three multi-material radiative heat transfer problems. One innovative idea of our work is that we introduce the

* This work was partially supported by NSFC Project (Grant No. 11031006, 91130002, 11171281), the Key Project of Scientific Research Fund of Hunan Provincial Science and Technology Department (Grant No. 2011FJ2011), Hunan Provincial Natural Science Foundation of China (Grant No. 12JJ3010).

weighted geometric average method for disposing the multi-material element (Also it is called as the mixed element)

When computing the diffusion coefficient. Hence, we compare it with arithmetic and harmonic average methods. Numerical results verify that the new scheme is valid and agreeable.

Another good idea of our work is that, we consider the effect of the convexity of nonlinear diffusion functions in mixed elements, and present two ways: one way is to evaluate the diffusion function values for two different materials firstly, and to take some average on two computed function values secondly; the other way is in the opposite order. Numerical results show that the stronger the convexity of diffusion function is, the more important the order of first averaging and second evaluating is, also show that the geometric average method is better than the harmonic one and in line with the arithmetic one for the strong convexity. The result above can be generalized to the higher dimensional problems, although the discussion is confined to one-dimensional case.

The third fine idea of our work is that, we design a novel SFVE scheme with the geometric average method based on the work in [8] for a two-dimensional multi-material radiative heat transfer problem. Numerical experiments show that the convergent order is less than two, and oscillates going with the oscillating proportion of the volume of some material in mixed elements. Based upon the above scheme, we construct a cylinder SFVE scheme for a three-dimensional heat transfer problem by transferring it to a two-dimensional one with the axis symmetry. Numerical experiments exhibit that numerical stimulations are valid and energy conservative errors are small and rational, and that it is convergent of order one when the backward Euler method is employed.

The remainder of this paper is organized as follows. In Section 2, we design a new finite volume scheme based on the geometric average method, and discuss the effect of the convexity of nonlinear diffusion functions. In Section 3, we construct a SFVE scheme for a two-dimensional multi-material radiative heat transfer problem. In section 4, we present a cylinder SFVE scheme for a three-dimensional problem and carry on some numerical experiments. Finally, we summarize our work in this paper.

## 2 THE GEOMETRY AVERAGE FINITE VOLUME SCHEME AND THE CONVEXITY OF DIFFUSION FUNCTION

In this section, we will consider the following nonlinear heat transfer problem

$$\begin{cases} \dfrac{\partial T}{\partial t} - \dfrac{\partial}{\partial x}(D\dfrac{\partial T}{\partial x}) = f(x), \quad a < x < b, 0 < t < t_{e,} \\ T(a) = T_1, T(b) = T_{2,} \end{cases} \tag{1}$$

where D is the nonlinear diffusion coefficient, such as $D = T^{\alpha}$. The variation of the diffusion coefficient may bring a fast moving wave front which is known as the Marskak wave [12].

### *2.1 The Finite volume Scheme*

Firstly, we take the uniform partition of the intervals [a,b] and [0, $t_e$], respectively,

$$a = x_0 < x_1 < ... < x_N = b, 0 = t_0 < t_1 < ... < t_N = t_e,$$

and denote

$$\Delta x = x_{i+1} - x_i, i = 0,1,2,..., N-1, \Delta t = t_{i+1} - t_i, i = 0,1,2,..., M-1.$$

In the following, the Crank-Nicolson scheme and a conservative second order finite volume scheme are applied to model problem 1 defined by Eq. (1). Hence, the numerical scheme is convergent of order two about space and time. The Jacobian-Free Newton Krylov method [11,13] is employed to the nonlinear part.

The time and space discretizations for Eq. (1) yield to

$$\frac{T_i - T_i^n}{\Delta t} - \frac{D_{i+1/2}(T_{i+1} - T_i) - D_{i-1/2}(T_i - T_{i-1})}{\Delta x^2} = f_i, \tag{2}$$

Where $T_i := T_i^{n+1} = T(x_i, t_{n+1}), D_{i+1/2}, D_{i-1/2}$ can be computed or approximated.

The following derivation is based on two assumptions: (1) we assume that the heat transfer coefficient is piecewise constant and continuous. (2) We consider steady state solutions. We can classify the elements as non-mixed elements and mixed elements. The non-mixed element means that there only one material in it, and the mixed element means that there are (at least) two materials in it. For example, in FIG.1, $[x_{i-2}, x_{i-1}]$ is a non-mixed element, and $[x_{i-1}, x_i]$ is a mixed element. For the former, $D_{i-3/2}$ can easily and uniquely be determined under above two conditions. However, for the latter, $D_{i-1/2}$ can only be approximated, i.e., it needs to be evaluated by some averaging, such as the arithmetic, harmonic or geometric averages. Now, we will focus on how to use three average methods for the computation of $D_{i-1/2}$ where the interface is shown as FIG. 1.

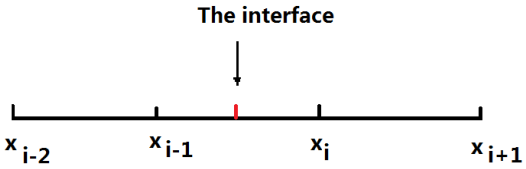


FIG. 1 THE INTERFACE AND GRID POINT

The arithmetic and harmonic average methods (See them in [6]) lead to

$$D^a_{i-1/2} = \frac{D_i + D_{i-1}}{2}, \tag{3}$$

and

$$D^h_{i-1/2} = \frac{2D_i D_{i-1}}{D_i + D_{i-1}}, \tag{4}$$

respectively.

The literature also shows that the truncation errors of above two methods are $O(\Delta x^2)$.

We can introduce another average method for computing $D^g_{i-1/2}$ i.e.,

$$D^g_{i-1/2} = \sqrt{D_i D_{i-1}}. \tag{5}$$

It is the well-known geometric average method.

From the literature [15], one can see that

$$D^h_{i-1/2} \le D^g_{i-1/2} \le D^a_{i-1/2},$$

and the truncation error of it is $O(\Delta x^2)$ obtained similarly to the literature [6]. The above relation means that the geometric average may be a agreeable one due to its immunity to the extreme values.

In the following, we will present some numerical experiments to display the characteristics of the geometric average method.

### *2.2 The Convexity of Diffusion Function and Numerical results*

In the section, we will display two numerical examples. One is from and more abundant than that in the literature [6]. We not only compare with three average methods, but also consider the convexity of the diffusion function $T^\alpha$. The other example is constructed where the exact solution is designed to verify the convergent order of three average methods.

**Example 1.** ([6]) We consider the model problem 1 defined by Eq. (1) with

$$[t_0, t_e]=[0,0.08],\ [a,b]=[0,1],\ f(x)=0,\ T(x,t_0)=0.1,\ T(a,t)=2.0,\ T(b,t)=0.1.$$

We not only present three cases of the diffusion coefficient $D = T^\alpha, \alpha = 1,3,6$, but also consider the convexity of the diffusion function $T^\alpha$. The approximation of $D_{i-1/2}$ can be obtained by the following two ways:

**(A)** Evaluate $T^\alpha_i, T^\alpha_{i-1}$, then take some average for them to get $D_{i-1/2}$.

**(B)** Take some average by $T_i, T_{i-1}$ to approximate $T_{i-1/2}$, then evaluate $(T_{i-1/2})^{\alpha}$.

Numerical results are shown as the figures from FIG.2 to FIG.4. The first two agree with those in the literature [6].

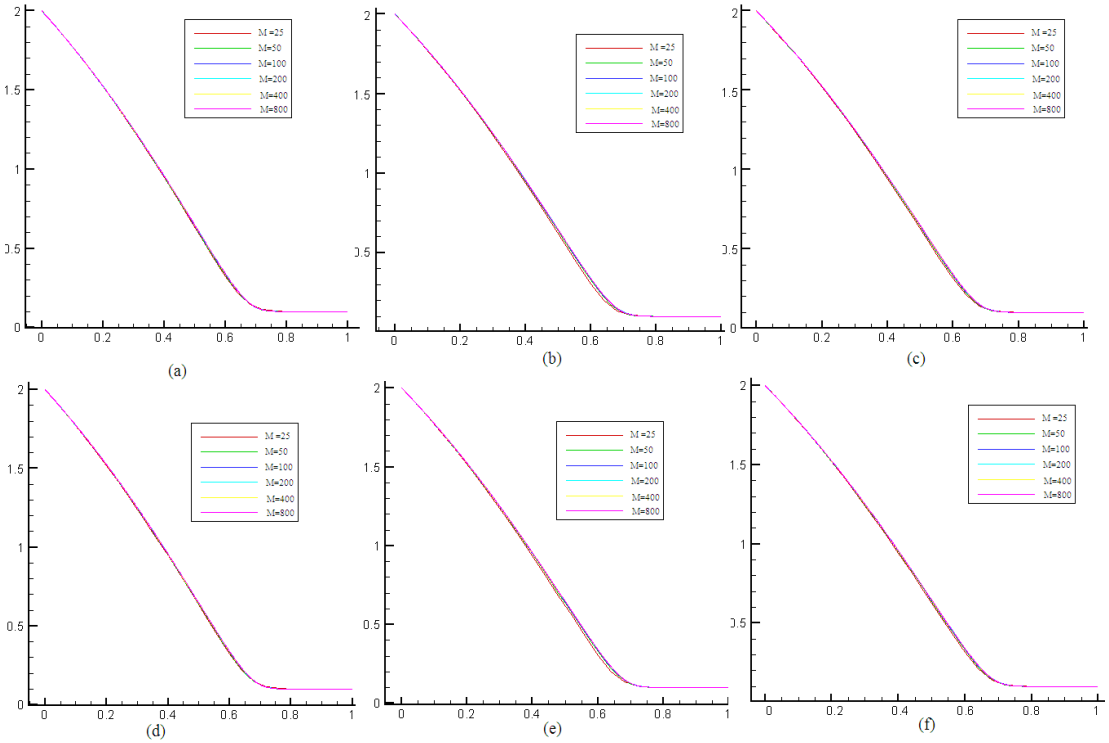


FIG. 2 COMPARISON FOR $\alpha = 1$: (A) ARITHMETIC. (B) HARMONIC. (C) GEOMETRIC. (D) F-ARITHMETIC. (E) F-HARMONIC. (F) F-GEOMETRIC.

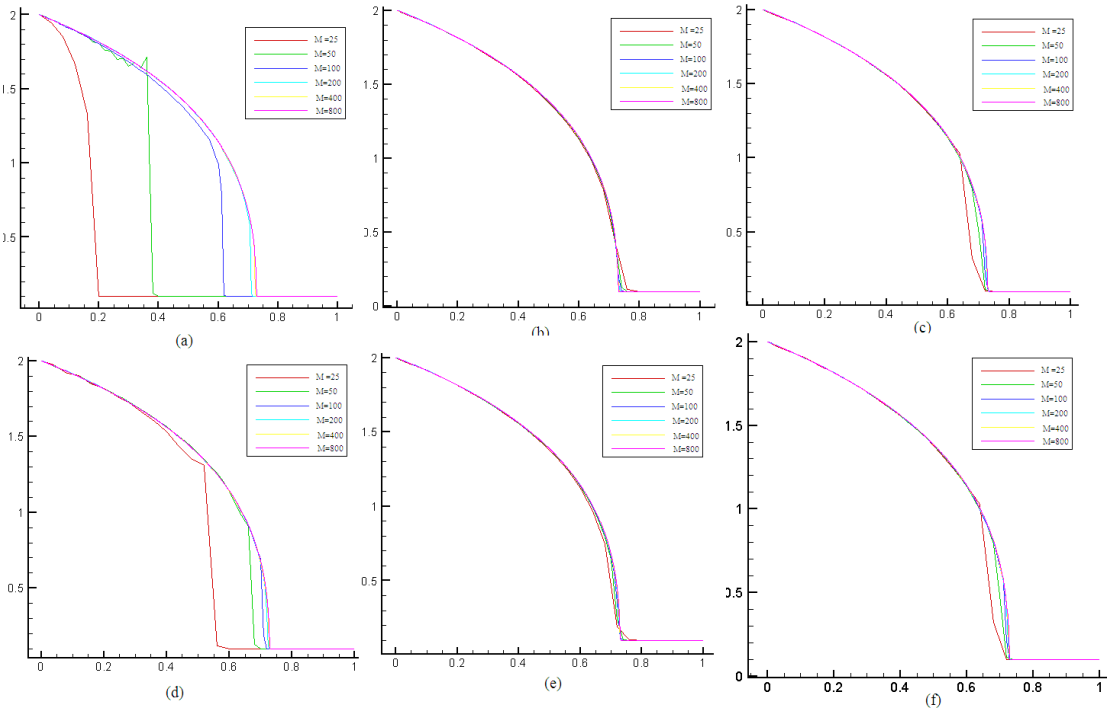


FIG. 3 COMPARISON FOR $\alpha = 3$: (A) ARITHMETIC. (B) HARMONIC. (C) GEOMETRIC. (D) F-ARITHMETIC. (E) F-HARMONIC. (F) F-GEOMETRIC.

In FIG.2, (A) (B) and (B) are the results for three averages (denoted as Arithmetic, Harmonic and Geometric) in the way **(A)**, respectively; and (d), (e) and (f) are also for three averages (denoted as f-Arithmetic, f-Harmonic and f-Geometric) in the way **(B)**, respectively. From this figure, one can see that, for D = T ($\alpha = 1$), the differences

between three average methods are very small.

From FIG.3, one can see that, for $D=T^3$ ($\alpha=3$) by above two approximate ways, the results are similar for harmonic and geometric average methods, but there is great difference for the arithmetic average method, and also can see that the way **(B)** is better than the way **(A)**.

From FIG.4, one can see that, for $D=T^6$ ($\alpha=6$), the differences are obviously great among three average methods. Firstly, the way **(B)** is better than the way **(A)**, especially for the harmonic average method. Secondly, the arithmetic average method is the best, the geometric one transfers moderately, however, the harmonic one transfers too slowly. Hence, as the $\alpha$ is big, one should be cautious to choose the harmonic average method.

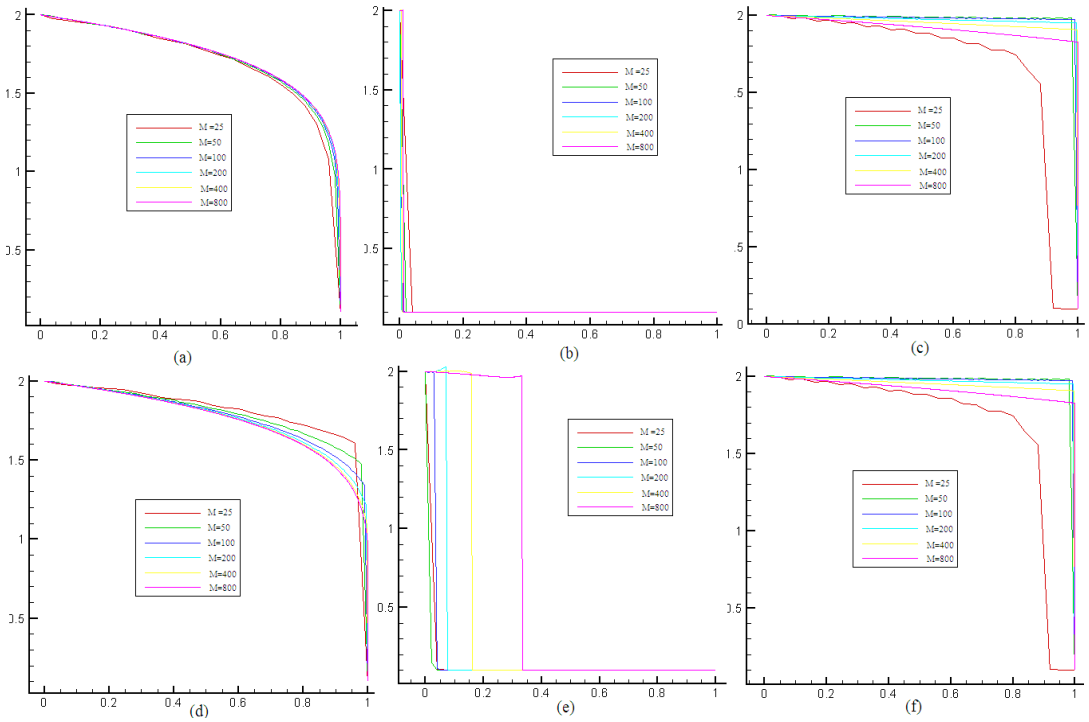


FIG. 4 COMPARISON FOR $\alpha=6$: (A) ARITHMETIC. (B) HARMONIC. (C) GEOMETRIC. (D) F-ARITHMETIC. (E) F-HARMONIC. (F) F-GEOMETRIC.

**Example 2.** We consider model problem 1 defined by Eq.(1), and take [a,b]=[$t_0$,$t_e$]=[0,1], $\alpha=4$ and the exact solution $T(x,t)=e^{\frac{t}{t+1}-x}$.

In this example, we employ above three average methods to compute $D_{i-1/2}$. The $L^2$-norms of the errors are shown as FIG.5 for approximate solutions at the moment $t_e=1$. From it, one can see that the convergent orders of three methods are all two, which agrees with that in the literature [6]. The error of the arithmetic one is the smallest, and that of the harmonic one is the biggest, which also is in accord with the relation (6).

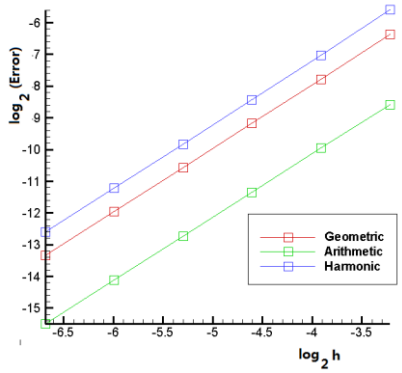


FIG. 5 COMPARISONS FOR CONVERGENT ORDERS.

# 3 A SYMMETRIC FINITE VOLUME ELEMENT SCHEME

In this section, we consider the following interface model problem

$$\begin{cases} -\nabla\cdot(\kappa\nabla u) = f, & x=(x_1,x_2)\in\Omega=\Omega_1\cup\Omega_2, \\ u=0, & x\in\partial\Omega, \end{cases} \tag{6}$$

where $f(x)\in L^2(\Omega)$, and $\kappa=\begin{cases}\kappa_0, & x\in\Omega_1,\\ 1, & x\in\Omega_2.\end{cases}$

## *3.1 SFVE SCHEME*

Assume that $\Omega_h=\{E_i,1\le i\le M\}$ is a quadrilateral partition for the region $\Omega$ (Shown as FIG.6). In this figure, the interface (the red solid line) leads to some mixed elements where the values of $\kappa$ cannot be determined accurately. We will construct a novel SFVE scheme based on the scheme in the literature [8] and the weighted geometric average method. The key idea of it is that the diffusion coefficient is approximated by some average value in a mixed element. We will display how the SFVE scheme is constructed as follows.

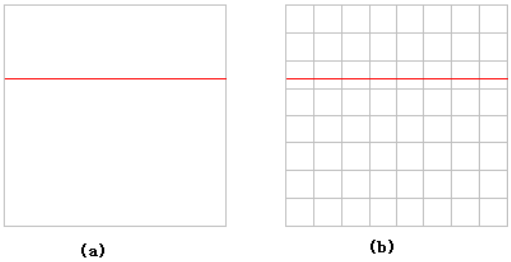


FIG. 6 THE PARTITION AND MIXED GRIDS.

**Step 1**: Obtain the element stiff matrix and load vector for any non-mixed element $E_i$ as the literature [8]

$$A^{E_i}=(a_{lm}^{E_i})_{4\times4}, F^{E_i}=(f_l^{E_i})_{4\times1}.$$

**Step 2**: Compute the approximate diffusion coefficient $\bar{\kappa}$ in the mixed element by the weighted geometric average method,

$$\bar{\kappa}=\kappa_1^{\chi}\kappa_2^{1-\chi}, \tag{7}$$

where $\chi$ is the proportion of the volume in the mixed element of $\kappa_1$, and $1-\chi$ is for $\kappa_2$.

**Step 3**: Get the corresponding element stiff matrix and load vector for the mixed element $E_i$,

$$a_{lm}^{E_i}=-\bar{\kappa}\int_{\overline{M_lO_kM_{l-1}}}\frac{\partial\varphi_{k_m}}{\partial n}ds,\ f_l^{E_i}=\int_{D_l}f dx, 1\le l,m\le4,$$

where $M_0=M_4$, $O_k$ and $D_l$ are the barycenter of the element and the sub-control volume about the vertex $X_{k_l}$, respectively (See FIG.7(a)).

**Step 4**: Assemble all the element stiff matrices and load vectors to total stiff matrix and load vector, i.e., to obtain the new scheme.

One can also compute $\bar{\kappa}$ by the following weighted arithmetic and harmonic average methods in **Step 2** to obtain the corresponding SFVE schemes

$$\bar{\kappa}=\chi\kappa_1+(1-\chi)\kappa_2, \tag{8}$$

$$\bar{\kappa}=\frac{1}{\chi/\kappa_1+(1-\chi)/\kappa_2}. \tag{9}$$

From above, one can see that the total stiff matrix is symmetric. Hence the new scheme is symmetric, which is helpful to increase the computational efficiency when solving the corresponding discrete system.

## *3.2 NUMERICAL EXPERIMENTS*

Now, we will present some numerical experiments for the new scheme.

**Example 3.** In model problem 2 defined by Eq. (6), we choose $\Omega=(0,1)^2$,

$\Omega_1=\{(x_1,x_2),0<x_1<1,0<x_2<2/3\}$, $\Omega_2=\{(x_1,x_2),0<x_1<1,2/3<x_2<1\}$, the interface $x_2=2/3$, $\kappa_0=16$ and

$$u(x_1,x_2)=\begin{cases}\sin(4\pi x_1)\sin(4\pi x_2)+2, & x\in\Omega_1,\\ \sin(4\pi x_1)\sin(16\pi x_2) & x\in\Omega_2.\end{cases}$$

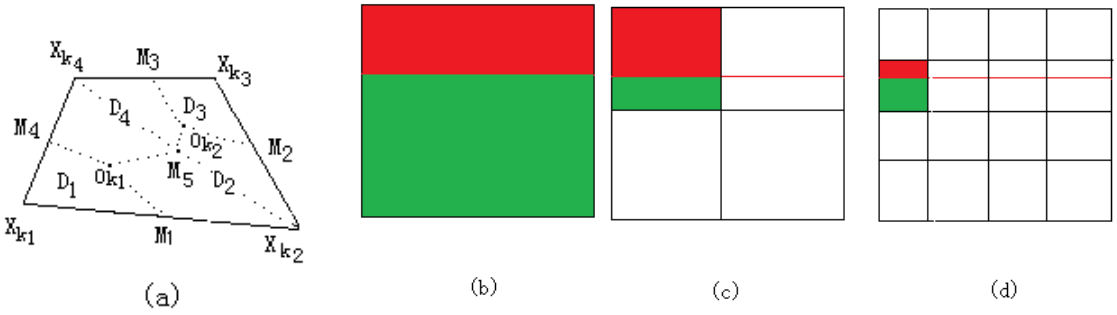


FIG. 7 (A) THE SUB-CONTROL VOLUMES. (B), (C) AND (D): THE OSCILLATION OF THE VOLUME PROPORTION.

Numerical results are shown in TABLE. 1, where $N_i, i=1,2$ is the partition number along the $x_i$-axis direction, respectively, and $\gamma$ is the ratio of error of the approximations for two partition step sizes h, h/2, $e_h=\|u-u_h\|_0$. From it, one can see that the convergent orders for three weighted average methods (Arithmetic, Harmonic and Geometric) are all less than two, and the errors of approximation $u_h$ seem oscillating when the grids are refined. It is due to the oscillation of the proportion of the volume of some material in the mixed element. The oscillation of the proportion is shown as FIG.7 (b) to (d). In addition, the oscillation of the geometric average is the smallest among the three methods; maybe it is the advantage of this average immune to the extreme value.

TABLE 1 THE $L^2$-ERROR FOR THREE AVERAGE METHODS.

| | Arithmetic | | Harmonic | | Geometric | |
|---|---|---|---|---|---|---|
| $N_1\times N_2$ | $e_h$ | $\gamma$ | $e_h$ | $\gamma$ | $e_h$ | $\gamma$ |
| 16 | 1.62e-1 | | 1.44e-1 | | 1.52e-1 | |
| 32 | 8.61e-2 | 1.88 | 9.73e-2 | 1.48 | 1.04e-2 | 1.46 |
| 64 | 2.43e-2 | 3.54 | 1.82e-2 | 5.34 | 2.25e-2 | 4.62 |
| 128 | 1.44e-2 | 1.69 | 1.65e-2 | 1.11 | 1.69e-2 | 1.33 |
| 256 | 4.86e-3 | 2.96 | 3.86e-3 | 4.27 | 4.60e-3 | 3.67 |

## 4 A SFVE SCHEME IN THE CYLINDER COORDINATE SYSTEM

In this section, we consider the following radiative heat transfer model problem ([14])

$$\begin{cases} c_e\rho\dfrac{\partial T_e}{\partial t}-\nabla\cdot(K_e\nabla T_e)=\rho W_{ei}(T_i-T_e)+\rho W_{er}(T_r-T_e),\\ c_i\rho\dfrac{\partial T_i}{\partial t}-\nabla\cdot(K_i\nabla T_i)=\rho W_{ei}(T_e-T_i),\\ 4aT_r^3\dfrac{\partial T_r}{\partial t}-\nabla\cdot(K_r\nabla T_r)=\rho W_{er}(T_e-T_r),\end{cases} \tag{10}$$

where the region $\Omega=\{(R,\theta,Z):0\le R\le R_0,0\le\theta\le 2\pi,0\le Z\le Z_0\}$ (shown as FIG.8 (a)) is divided two parts filled with two different materials: plastic foam (CH) and deuterium gas (DT), respectively, and ...

The model problem 3 defined by Eq. (10) approximately describes the process of radiant energy broadcasting in the quiescent medium and energy exchange of electrons with photons and ions whose temperatures are denoted as $T_e, T_r$ and $T_i$, respectively.

In this section, we only consider the Z-axis-symmetric problem, so $T_e, T_i$ and $T_r$ are all irrelative to the angle variable $\theta$. Hence, we need to solve the model problem 3 defined by Eq. (10) on some section region (also denoted as $\Omega$) shown as FIG.8 (b).

In above equations (10),

(i) $W_{ei} = \rho A_{ei} T_e^{-3/2}$ and $W_{er} = \rho A_{er} T_e^{-1/2}$ are the energy exchange coefficients between electron and ion, and between electron and photon, respectively;

(ii) $K_\alpha = A_\alpha T_\alpha^{5/2}, \alpha = e,i; K_r = 3\times 10^6 l_r T_r^{3+\beta}$ are the diffusion coefficients about electron, ion and photon, respectively;

(iii) $c_e = 1.5\Gamma_e, c_i = 1.5\Gamma_i, c_r = 4aT_r^3$ are the thermal capacities about electron, ion and photon, respectively.

In above physical parameters, $A_{ei}, A_{er}, A_e, A_i, l_r, \beta, \Gamma_e, \Gamma_i, a$ are different constants in different sub-domains, and $\rho$ is the density of materials.

### *4.1 SFVE SCHEME*

Assume that a quadrilateral partition $\Omega_h$ is shown as FIG.8 (c). The interface line (red solid line) leads to some mixed elements. A non-mixed element and a mixed element are shown as (d) and (e), respectively. We take the backward Euler method for discretizing the time direction to obtain the nonlinear elliptic equations, then employ the "fixed-coefficient" (Picard) method for the linearization to get the linear elliptic equations. Now, we come to construct a SFVE scheme for the linear elliptic equations on $\Omega_h$, and present how to design the scheme.

**Step 1**: Compute the proportions of the volume and mass about two materials in mixed elements where the mass proportions are denoted as $\chi_i, i = 1,2$, and compute the approximate physical parameters by the mass proportions.

(i) The thermal capacities $c_\alpha, \alpha = e,i$, the material densities and the energy exchange coefficients are approximated by the weighted arithmetic average method.

(ii) The atomic weight $A_\alpha, \alpha = e,i,r$, the Rosseland of photon $l_r = A_r \rho^m T_r^n$ are approximated by the weighted harmonic average method.

**Step 2**: Compute the approximate diffusion coefficients by the weighted geometric average methods in the direction of R and Z after obtaining the corresponding limited flux diffusion coefficients, denoted as $\overline{K}_i^R, \overline{K}_i^Z, i = 1,2,3$ for $T_e, T_i$ and $T_r$, respectively.

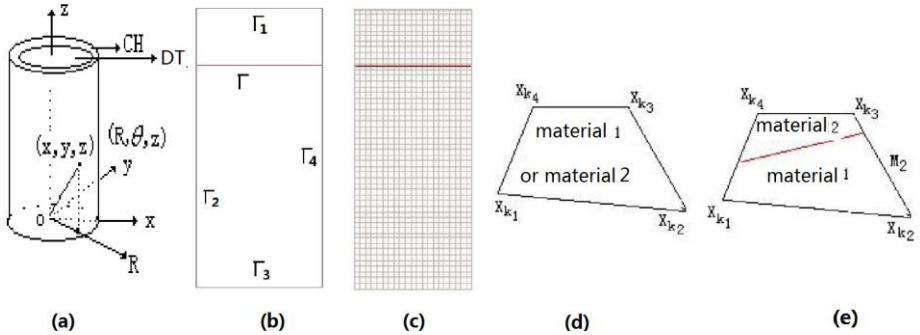


FIG. 8 (A) THE REGION $\Omega$. (B)THE SECTION REGION $\Omega$ (B) MIXED GRIDS. (C) A NON-MIXED ELEMENT. (D) A MIXED ELEMENT.

**Step 3**: Present the element stiff matrix and load vector for any mixed element E

$$A^E = (a_{lm})_{4\times 4}, F^E = (f_l)_{4\times 1},$$

where

$$a_{lm} = \begin{cases} (d^{ll})_{3\times 3}, & l = m, \\ (b^{lm})_{3\times 3}, & l \neq m. \end{cases}$$

When $1 \le l, m \le 4$ and $l \ne m$, we have

$$(b^{lm})_{3\times 3} = -2\pi\Delta t\{\int_{L_l} \frac{\partial \phi_{k_m}}{\partial R}\cos\theta_l R ds \begin{bmatrix} \overline{K}_1^R & 0 & 0 \\ 0 & \overline{K}_2^R & 0 \\ 0 & 0 & \overline{K}_3^R \end{bmatrix} + \int_{L_l} \frac{\partial \phi_{k_m}}{\partial Z}\sin\theta_l R ds \begin{bmatrix} \overline{K}_1^Z & 0 & 0 \\ 0 & \overline{K}_2^Z & 0 \\ 0 & 0 & \overline{K}_3^Z \end{bmatrix}\},$$

where $(\cos\theta_l, \sin\theta_l)$ is the unit outer normal vector $n_l$ on the control-volume boundary $L_l$, $\phi_{k_m}$ is the nodal linear basis function about the vertex $X_{k_m}$;

When $1 \le l, m \le 4$ and $l = m$, we have

$$(d^{ll})_{3\times 3} = (b^{ll})_{3\times 3} + 2\pi\int_{D_l}\{\begin{bmatrix} a_e & 0 & 0 \\ 0 & a_i & 0 \\ 0 & 0 & a_r \end{bmatrix} + \Delta t \begin{bmatrix} d_{ei}+d_{er} & -d_{ei} & -d_{er} \\ -d_{ei} & 0 & 0 \\ -d_{er} & 0 & 0 \end{bmatrix}\} R dR dZ,$$

$$f_l = 2\pi\int_{D_l} \begin{bmatrix} f_e \\ f_i \\ f_r \end{bmatrix} R dR dZ,\ 1 \le l \le 4,$$

where $f_\alpha, \alpha = e, i, r$ are the right sides of above linearized elliptic equations about $T_\alpha$, respectively.

**Step 4**: Compute the element stiff matrices and load vectors for non-mixed elements.

**Step 5**: Assemble all the element stiff matrices and load vectors to obtain the total stiff matrix and load vector.

From above, one can see that the total stiff matrix is symmetric. Hence, we have obtained a new SFVE scheme based on the weighted geometric average method for this three-dimensional model problem. The symmetry is also helpful to increase the computational efficiency when solving the corresponding discrete systems.

One can also compute $\overline{K}_i^R, \overline{K}_i^Z, i = 1,2,3$ by the weighted arithmetic and harmonic average methods in **Step 2** to obtain the corresponding SFVE schemes.

### *4.2 Numerical Experiments*

In this subsection, we carry on some numerical experiments.

**Example 4.** In the model problem 3 defined by Eq. (10), we choose $\Omega = (0,30)\times(0,95)$ the interface $\Gamma$ : Z=74.1, the proper physical parameters, and the proper boundary conditions

$$\frac{\partial T_\alpha}{\partial n}\Big|_{\Gamma_2\cup\Gamma_2\cup\Gamma_4} = 0, \alpha = e, i, r; \frac{\partial T_\nu}{\partial n}\Big|_{\Gamma_1} = 0, \nu = e, i; T_r\Big|_{\Gamma_1} = 2,$$

and the initial-value condition $T_\alpha\big|_{t=0} = 3\times 10^{-4}, \alpha = e, i, r;$ and $[t_0, t_e] = [0,30]$, the unit of time is 0.1 ns.

We take the uniform partition $\Omega_h$, the partition numbers along R-axis and Z-axis directions are 30 and 96, respectively. We refine a line of grids neighboring to the radiative temperature boundary (Dirichlet boundary on $\Gamma_1$) to decrease the energy conservative error. Hence, step sizes of R-axis and Z-axis are almost one unit.

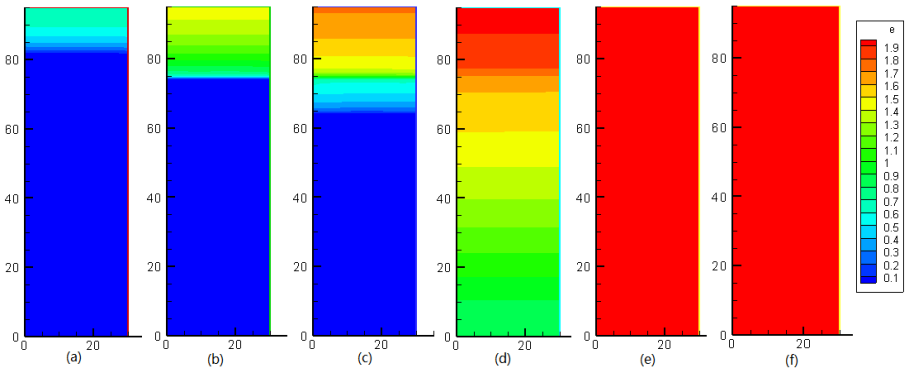

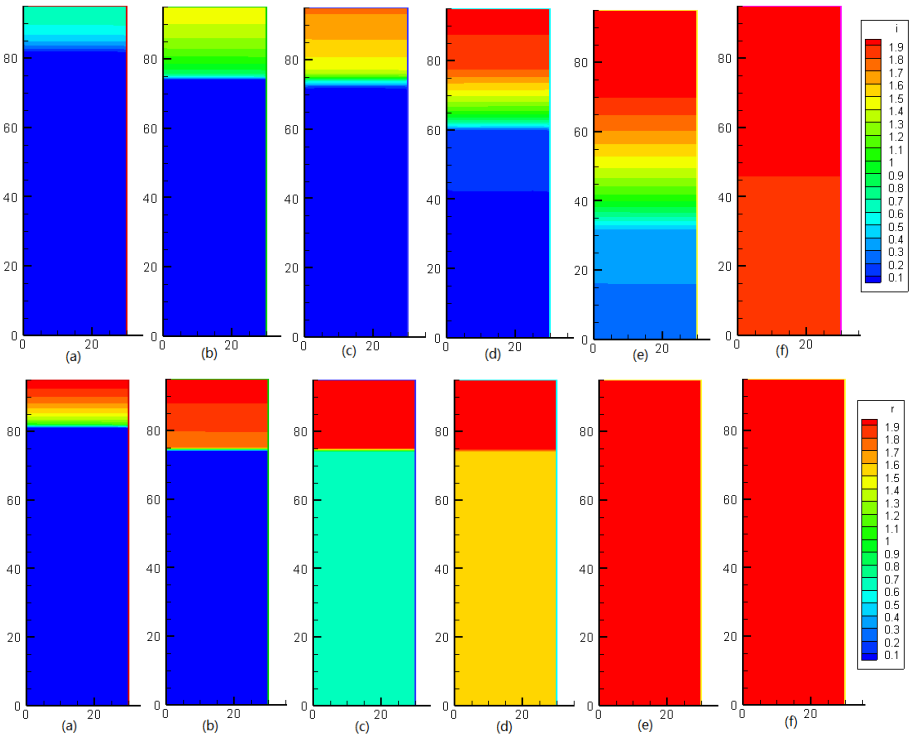

FIG. 9 THE TEMPERATURE DISTRIBUTIONS FOR GEOMETRIC AVERAGE METHOD AT SIX MOMENTS:

TOP FOR TE. MIDDLE FOR TI. BOTTOM FOR TR.

Firstly, we consider the weighted geometric average method. Numerical results are shown in FIG.9. From FIG.9 (top) to FIG.9 (bottom), one can see that the transfers of electron, iron and photon agree with the real physical phenomena. Simultaneously, the energy conservative error is less than 3% (Shown as the red solid curve in FIG.12 (a). The followings are also the red solid curve).

Then, we consider the weighted harmonic average method. Numerical results are shown in FIG.10. From FIG.10 (top) to FIG.10 (bottom), one can see that the transfers of electron, iron and photon also agree with the real physical phenomena. Simultaneously, the energy conservative error is less than 3% (Shown as FIG.12 (b))

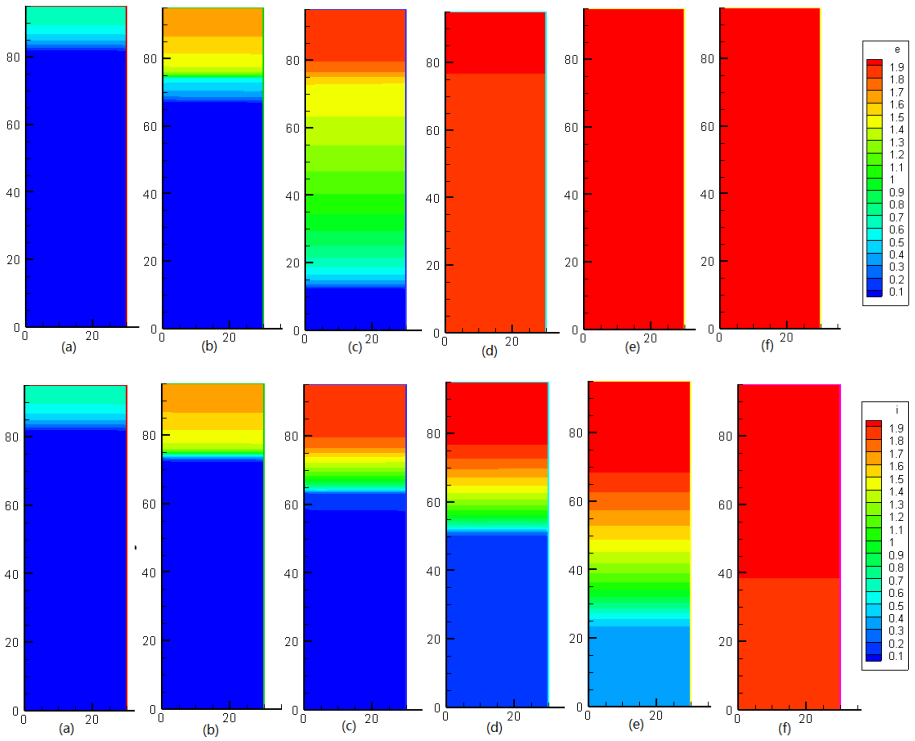

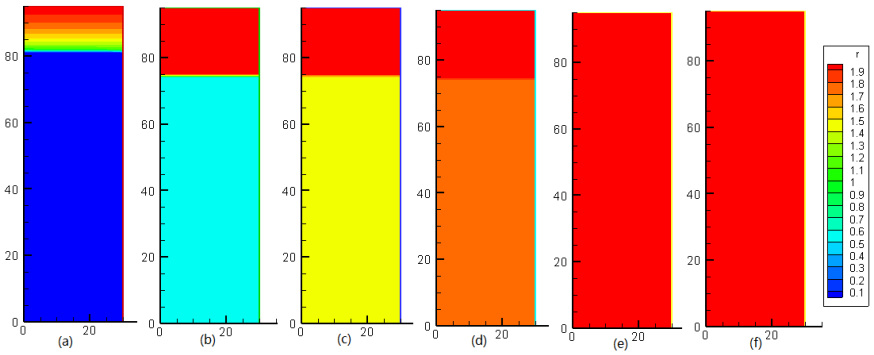

FIG. 10 THE TEMPERATURE DISTRIBUTIONS FOR HARMONIC AVERAGE METHOD AT SIX MOMENTS: UPPER FOR TE. MIDDLE FOR TI. BOTTOM FOR TR.

Finally, we consider the weighted arithmetic average method. Numerical results are shown in FIG. 11. In the figures for temperature distributions, the horizontal and vertical axes are Z-axis and R-axis, respectively. From FIG. 11 (top) to FIG. 11 (bottom) respectively, one can see that the transfers of electron, iron and photon agree with the real physical phenomena. Simultaneously, the energy conservative error is less than 3% (Shown as FIG.12 (c)).

Furthermore, we refine the mesh above, obtain the corresponding errors and display in FIG.12 (see the blue solid line). Comparing the red solid line with the blue one, one can also see that the energy conservative errors all reduce by 50% for three weighted average methods.

Comparing with all figures above carefully, one can find the following facts.

(1) According to the small energy conservative error, the numerical simulation is agreeable for weighted geometric average method. So do the other two average methods.

(2) For $T_r$ and $T_e$, there are few differences between the weighted geometric and arithmetic averages. The transfers simulated by the weighted harmonic average are faster than those of the other two averages. It is due to the characteristic property of this average method, i.e., the average value is partial to that in the small proportion region.

In this experiment, the higher temperature lies in the small proportion region in the mixed elements, which leads to the bigger diffusion coefficients. Maybe it is the defect of the harmonic average method not immune to the extreme value.

(3) For $T_i$, there are few differences among three averages. It can be understood by the fact that the process of energy exchange is: from $T_r$ to $T_e$, then from $T_e$ to $T_i$, together with the character of the energy exchanges' coefficients.

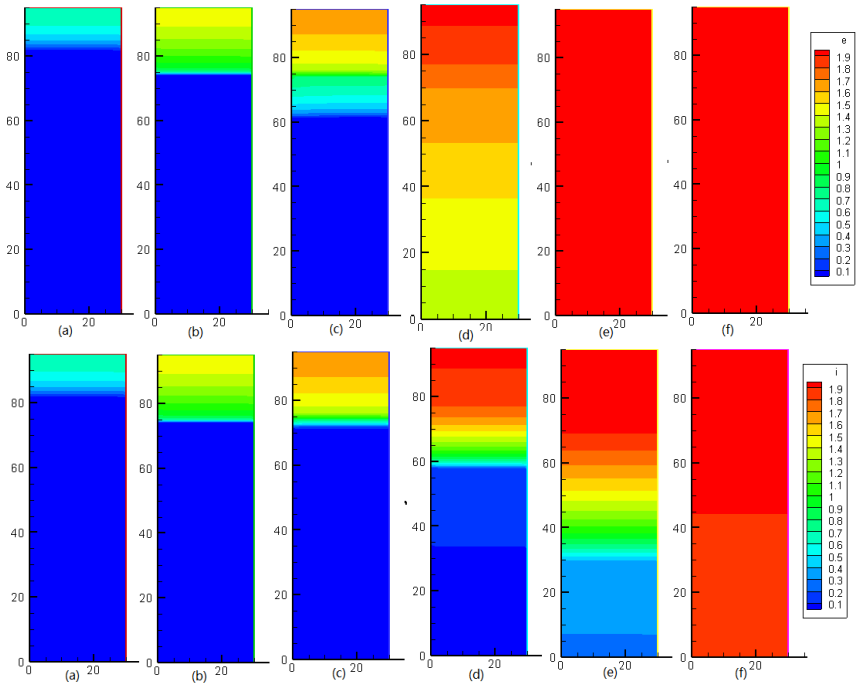

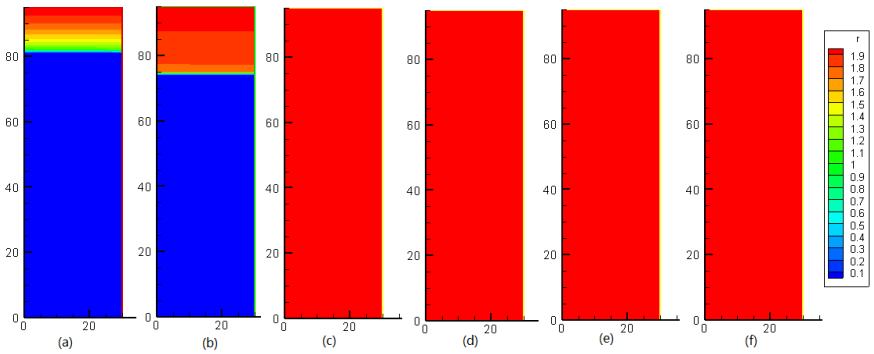

FIG. 11 THE TEMPERATURE DISTRIBUTIONS FOR ARITHMETIC AVERAGE METHOD AT SIX MOMENTS: UPPER FOR TE. MIDDLE FOR TI . BOTTOM FOR TR.

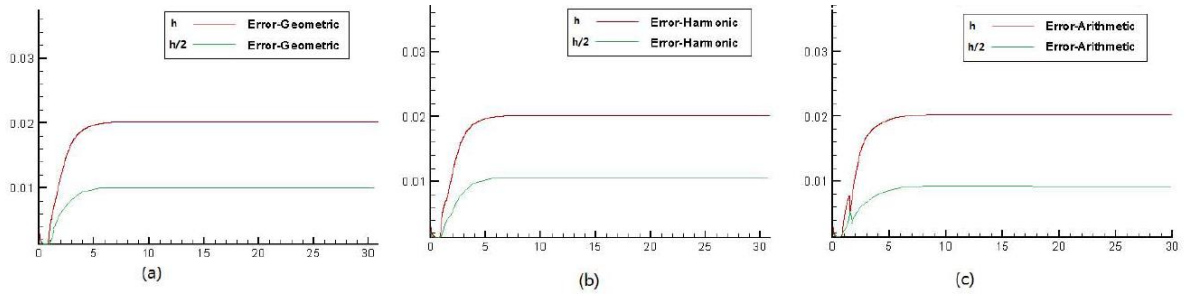


FIG. 12 THE COMPARISON FOR ENERGY CONSERVATIVE ERRORS OF THE THREE AVERAGE METHODS.

## 5 CONCLUSIONS

In this paper, we construct a novel finite volume scheme for solving three multi-material radiative heat transfer problems. We innovatively introduce the weighted geometric average method for disposing the diffusion coefficient in the mixed element, and take the effect of the convexity of nonlinear diffusion functions into account. Numerical results confirm that the new scheme is valid and agreeable.


## ACKNOWLEDGMENT

The authors thank Prof. Shi Shu and Dr. Chunsheng Feng for many helpful discussions.


## REFERENCES


[1] A. Jafari, S.H. Seyedein and M. Haghpanahi, Modeling of heat transfer and solidification of droplet/substrate in microcasting SDM process, International Journal of Engineering Science,18(2008): 187-198

[2] C. L. Zhai, W.B. Pei, Q.H, Zeng. 2D LARED-H simulation of ignition hohlraum, In Proc. the World Congress on Engineering 2010(III) WCE 2010, London, U.K

[3] H. B. James, J.T. King, A finite element method for interface problems in domains with smooth boundaries and interfaces, Adv. Comp. Math., 6(1996): 109-138

[4] Z. M. Chen, J. Zou, Finite element methods and their convergence for elliptic and parabolic interface problems, Numer. Math., 79(1998): 175-202

[5] S.V. Patankar. Numerical heat transfer and fluid flow. Hemisphere, New York, (1980)

[6] S.Y. Kadioglu, R. R. Nourgaliev and V. A. Mousseau, A comparative study of the harmonic and arithmetic averaging of diffusion coefficients for nonlinear heat transfer problem, Idaho National Laboratory, March, 2008

[7] S.B. Yuste, Weighted average finite difference methods for fractional diffusion equations, Journal of Computational Physics 216(2006): 264-274

[8] C. Y. Nie, S. Shu, Z.Q. Sheng, A Symmetry-preserving finite volume element scheme on unstructured quadrilateral grids, Chinese J. Comp. Phys. 26(2009): 17-22

[9] A. G. Hansen, M.P. Bendsoe, and O. Sigmund. Topology optimazation of heat transfer problems using the finite volume method. Struct.Multidisc. Optim, 31(2006): 251-259

[10] G. L. Olson and J. E. Morel. Solution of the radiation diffusion equation on an AMR eulerian mesh with material interface. In Technical Report LA-UR-99-2949, 1999. Los Alamos National Laboratory

[11] D. A. Knoll and D. E. Keyes. Jacobien-free newton krylov methods: a survey of approaches and applications. J. Comput. Phys., 4(2004): 357-397

[12] R.E. Marshak, Effect of radiation on shock wave behavior, Phys. Fluids, 1(1958): 24-29

[13] J.Y Yue, G.W. Yuan, Z.Q. Sheng, Picard-Newton iterative method for multimaterial nonequilibrium radiation diffusion problem on distorted quadrilateral meshes in: Proc. the World Congress on Engineering (II), WCE 2009, London, U.K

[14] C.Y. Nie, S. Shu, X.D. hang and J. Chen, SFVE schemes for radiative heat transfer problems in cylindrical coordinates and numerical simulation, Journal of System Simulation, 24(2012): 275-283

[15] S. Toader and G. Toader, Symmetries with Greek means, Creative Math. 13(2004): 17-25

## AUTHORS

[1]***Cunyun Nie*** (1974- ), Doctor Degree, associate professor, major in computational mathematics, major field of study: numerical computation and numerical stimulation for heat transfer and fluid dynamics.

[2] ***Haiyuan Yu*** (1962- ), Doctor Degree, professor, major in computational mathematics, major field of study: numerical computation and numerical stimulation and super-convergence for FEM.